



Environment and
Climate Change Canada

Environnement et
Changement climatique Canada

Canada



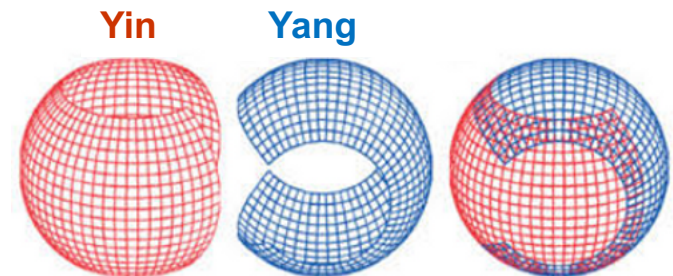
Global Environmental Multiscale model with a new terrain-following vertical coordinate based on height

Syed Zahid Husain, Claude Girard, Abdessamad
Qaddouri, André Plante

RPN-A, Meteorological Research Division
Environment and Climate Change Canada, Dorval, QC, Canada

The Global Environmental Multiscale (GEM) Model

- Principal features of the GEM dynamical core include
 - log-hydrostatic-pressure-type terrain-following vertical coordinate,
 - two time-level iterative implicit temporal discretization,
 - semi-Lagrangian advection,
 - Charney-Phillips grid in the vertical, and
 - Arakawa C-grid in the horizontal.
- The global horizontal discretization is based on an Yin-Yang type grid.



Motivations for the New Core

- Pressure-based vertical coordinate allows use of fast a direct solver for the discretized elliptic problem. However, it
 - loses scalability for large number of processor cores, and therefore,
 - necessitates development of efficient iterative solvers.
- The pressure-based dynamical core exhibits prohibitive numerical instability for steep orography (slope $> 45^\circ$) .
 - Adversely affects the sub-kilometer forecasting systems over complex orography.
- Overall, a **height-based dynamical core** is expected to be
 - more amenable to iterative solvers, and
 - may improve steep orography-related instability.

Height-based Vertical Coordinate in GEM

- A height-based **SLEVE**-like (Schär et al., 2002) terrain-following vertical coordinate, defined as

$$z = \zeta + B_1 z_{sL} + B_2 (z_s - z_{sL})$$

is adopted, where ζ is the terrain-following coordinate, z is the true height, z_s is the height of the surface, and z_{sL} stands for large-scale orography.

- The terms B_1 and B_2 determine the rate of flattening of the large- and fine-scale orographic imprints on the terrain-following coordinate with increasing altitude, defined as

$$B = \left(\frac{\zeta_T - \zeta}{\zeta_T} \right)^r = \lambda^r \text{ where } r = [r_{max} - (r_{max} - r_{min})\lambda].$$

Quick Implementation Strategy

- From here on, we will refer to the new and the existing dynamical cores as **GEM-H** and **GEM-P**.
- In order to facilitate a **quick implementation** of the **GEM-H** dynamical core, we have
 - the same horizontal and vertical grids and discretization as in GEM-P,
 - employed the same (or corresponding) prognostic variables,
 - the same semi-Lagrangian approach for advection, and
 - applied the same two-time-level implicit iterative temporal discretization.



Model Formulation: GEM-H

- **GEM-H** formulation utilizes an isothermal basic state, defined by temperature T_* and pressure p_* , connected through the hydrostatic relation, i.e., $\frac{\partial \ln p_*}{\partial z} = -g/RT_*$.
- We have **five prognostic equations for five variables**, namely, $\mathbf{V} = (u, v, w)$, T , and q [where $q = RT_* \ln(p/p_*)$].
- **Transformation from z to ζ coordinate** requires

$$\frac{\partial}{\partial X_z} \equiv \frac{\partial}{\partial X} - \frac{J_X}{J_\zeta} \frac{\partial}{\partial \zeta}; \quad \frac{\partial}{\partial Y_z} \equiv \frac{\partial}{\partial Y} - \frac{J_Y}{J_\zeta} \frac{\partial}{\partial \zeta}; \quad \frac{\partial}{\partial z} \equiv \frac{1}{J_\zeta} \frac{\partial}{\partial \zeta}; \quad \frac{\partial}{\partial t_z} \equiv \frac{\partial}{\partial t}$$

where

$$J_X = \frac{\partial z}{\partial X}, \quad J_Y = \frac{\partial z}{\partial Y}, \quad \text{and} \quad J_\zeta = \frac{\partial z}{\partial \zeta}.$$

Dynamical System of Eqn.

$$\frac{du}{dt} - \left(f + \frac{\tan\theta}{a} u \right) v + \frac{T}{T_*} \left(\frac{\partial q}{\partial X} - \frac{J_X}{J_\zeta} \frac{\partial q}{\partial \zeta} \right) = 0$$

$$\frac{dv}{dt} + \left(f + \frac{\tan\theta}{a} u \right) u + \frac{T}{T_*} \left(\frac{\partial q}{\partial Y} - \frac{J_Y}{J_\zeta} \frac{\partial q}{\partial \zeta} \right) = 0$$

$$\frac{dw}{dt} + \frac{T}{T_*} \left(\frac{1}{J_\zeta} \frac{\partial q}{\partial \zeta} - g \frac{T'}{T} \right) = 0$$

$$\frac{d}{dt} \left[\ln \left(\frac{T}{T_*} \right) - \frac{q}{c_p T_*} \right] + \frac{N_*^2}{g} \mu w = 0$$

$$\frac{d}{dt} \left(\frac{q}{c_*^2} + \ln J_\zeta \right) + \frac{\partial u}{\partial X} + \frac{1}{\cos\theta} \frac{\partial(\cos\theta v)}{\partial Y} + \frac{\partial \dot{\zeta}}{\partial \zeta} - \frac{g}{c_*^2} w = 0$$

$$\frac{d}{dt} (z - \zeta) + \dot{\zeta} - w = 0$$

Momentum equations

Thermodynamic equation

Continuity equation

Kinematic equation

where, $T' = T - T_*$, $N_*^2 = g^2 / c_p T_*$, and $c_*^2 = RT_* / (1 - \kappa)$.

Temporal Discretization

- Individual equations have the form

$$\frac{dF}{dt} + G = 0,$$

and are discretized in time using a two-time level Crank-Nicholson scheme as

$$\frac{F_A^+ - F_D^-}{\Delta t} + \underbrace{bG_A^+ + (1-b)G_D^-}_{\text{off-centered averaging}} = 0.$$

$$[b \geq 0.5]$$

A: arrival points
D: depart. locations

- Differential off-centering:** Three off-centering parameters:
 - b_m for the horizontal momentum equations,
 - b_h for continuity and thermodynamic equations, and
 - b_{nh} for the vertical momentum equation.

Solution Approaches

- Individual equations are rearranged as

$$\left(\frac{F_A^+}{b\Delta t} + G_A^+ \right)_{linear} = \frac{F_D^-}{b\Delta t} - \left(\frac{1-b}{b} \right) G_D^- - \left(\frac{F_A^+}{b\Delta t} + G_A^+ \right)_{nonlinear}$$

- Through elimination of variable the system of equations is reduced to a single elliptic boundary value (EBV) problem.
- General form of the EBV** (for both **GEM-P** and **GEM-H**):

$$\nabla_H^2 P + M_{VH} P = R$$

where, the subscripts H and V indicate coefficients that vary in the horizontal and the vertical, and M_{VH} includes difference and mean operators in the horizontal and the vertical.

- Simplified approach:** Metric terms in the nonlinear part. Allows use of the fast **direct solver**.

Results



Environment and
Climate Change Canada

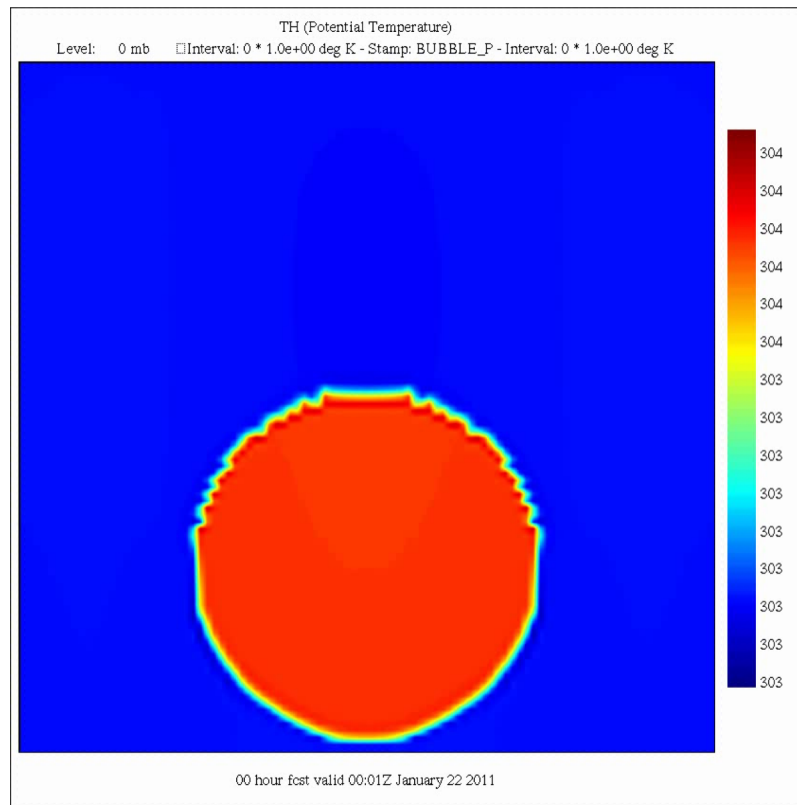
Environnement et
Changement climatique Canada

Canada 

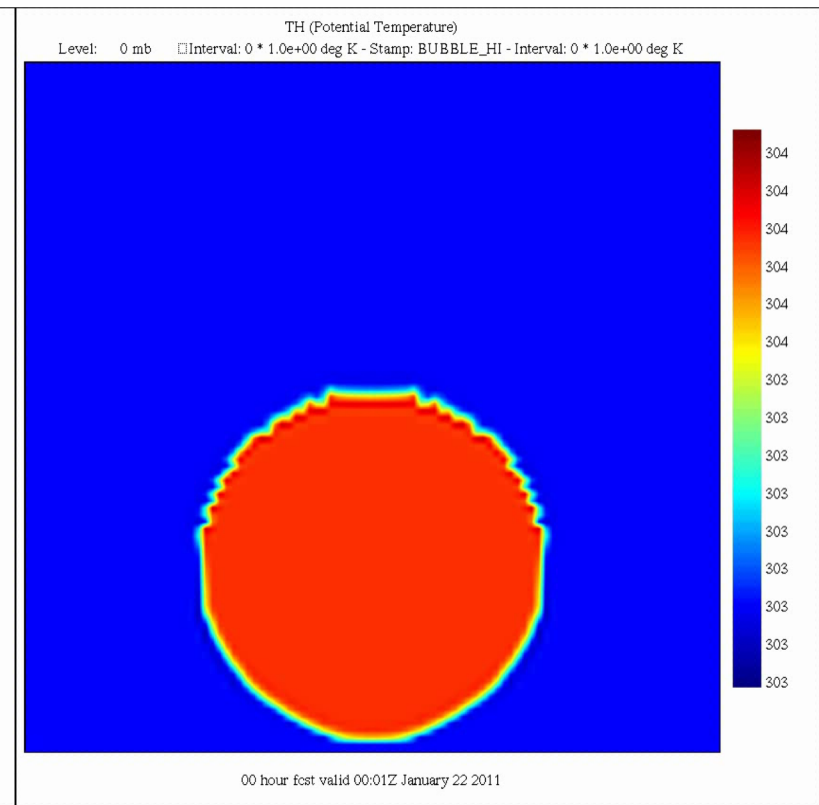
Robert's Bubble Convection Test

- Evolution of potential temperature distribution for a 500 m diameter bubble with an initial potential temperature excess of 0.5°C over an isentropic environment (Robert, 1993).

GEM-P



GEM-H

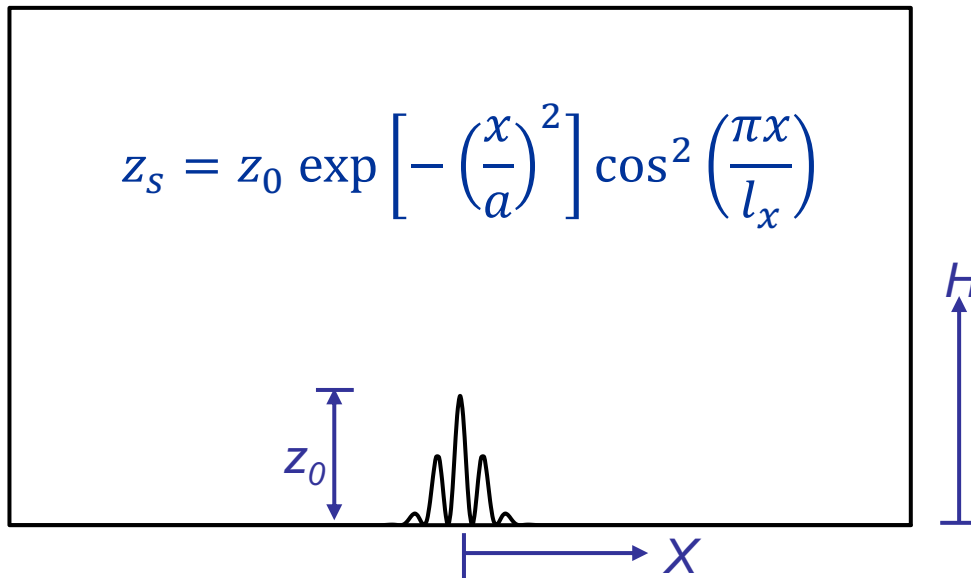


Robert, A. (1993): Bubble convection experiments with a semi-implicit formulation of the Euler equations. *J. of Atmos. Sciences*, 50: 1865-1873.

The Schär Mountain Case

A Theoretical Non-Hydrostatic Case

Schär case: Dry flow past idealized topography



$$U = 10 \text{ ms}^{-1}$$
$$N = 0.01 \text{ s}^{-1}$$
$$T_\theta = 288 \text{ k}$$

$$L = 200 \text{ km} \quad H = 19.5 \text{ km}$$
$$N_f = 401 \quad N_k = 65$$
$$\Delta x = 500 \text{ m} \quad \Delta z = 300 \text{ m}$$
$$z_0 = 250 \text{ m} \quad a = 5 \text{ km}$$
$$l_x = 4 \text{ km} = 8\Delta x$$

Schär, C., Leuenberger, D., Fuhrer, O., Lüthi, D., and Girard, C. (2002): A new terrain-following vertical coordinate formulation for atmospheric prediction models. *Mon. Wea. Rev.*, 130: 2459-2480.



The Schär Mountain Case

- A theoretical nonhydrostatic case.
- Dry adiabatic flow past idealized topography given by

$$z_s = z_0 \exp \left[- \left(\frac{x}{a} \right)^2 \right] \cos^2 \left(\frac{\pi x}{l_x} \right)$$

where $N_f=401$, $N_k=65$, $\Delta x=500$ m, $\Delta z=300$ m, $z_0 = 250$ m, $a = 5$ km, and $l_x = 4$ km = $8\Delta x$.

Also $U = 10$ ms⁻¹, $N = 0.01$ s⁻¹, and $T_\theta = 288$ k.

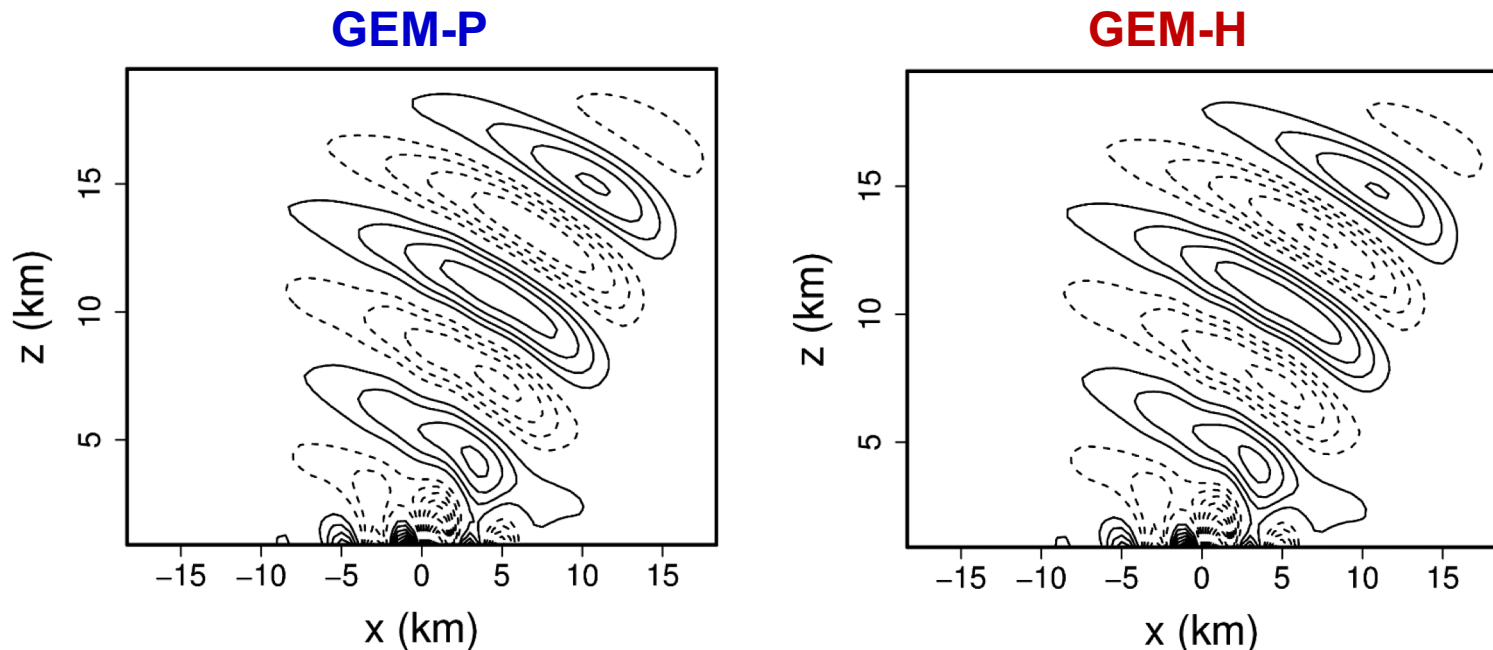


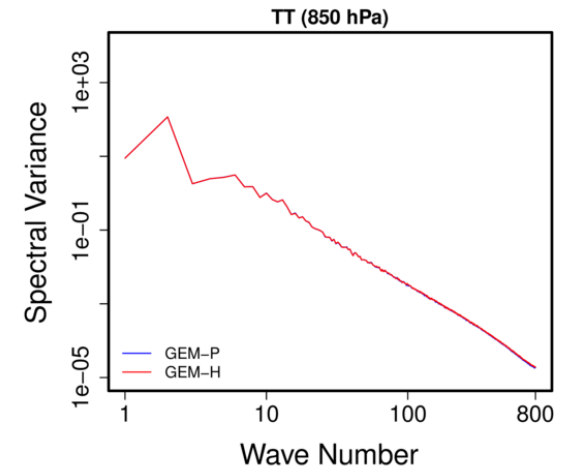
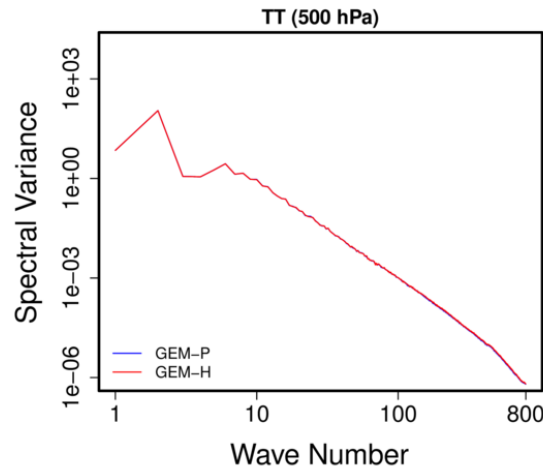
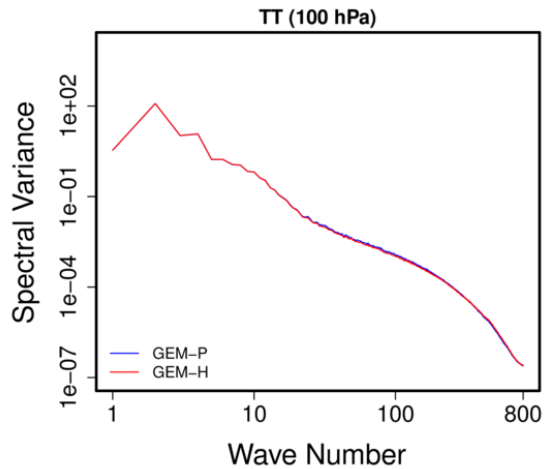
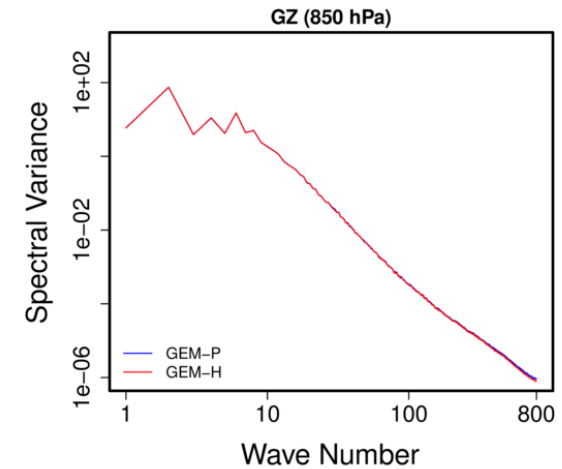
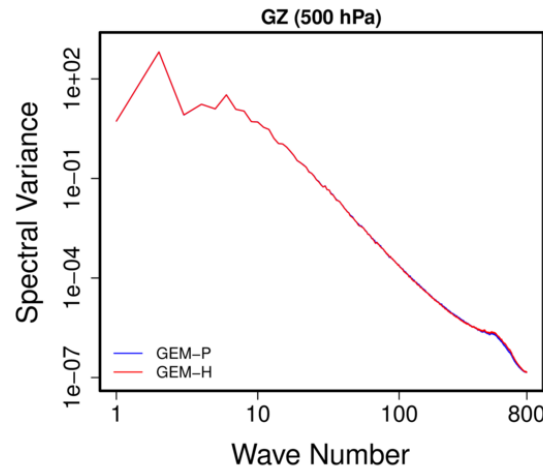
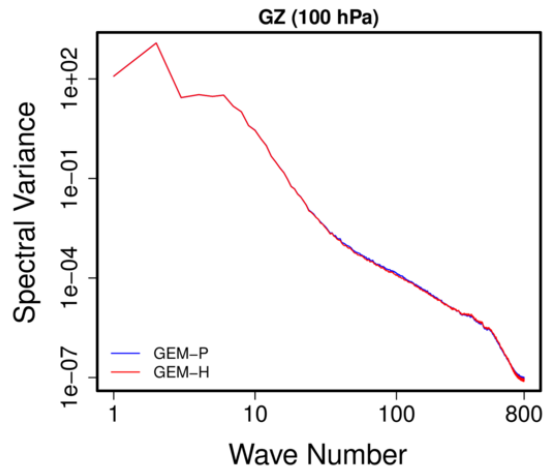
Fig: Vertical velocity contours with interval of 0.1 m s⁻¹

NWP Tests

- At present, we have a functional **GEM-H** dynamical core for both global and limited-area prediction systems.
- The RPN physics package has been coupled to the new dynamical core (without any additional calibration).
- Both direct and iterative solvers are available for **GEM-H**.
- At this point, our objective is to first produce forecasts with **GEM-H** that are equivalent of **GEM-P** for ECCO's different operational prediction system configurations.
- Tests have been conducted for the 25-km GDPS (Global Deterministic Prediction System) setup.
- Results are available for northern hemisphere winter and summer cases.

Variance Spectra

GEM-P vs **GEM-H** (T+120 hr)

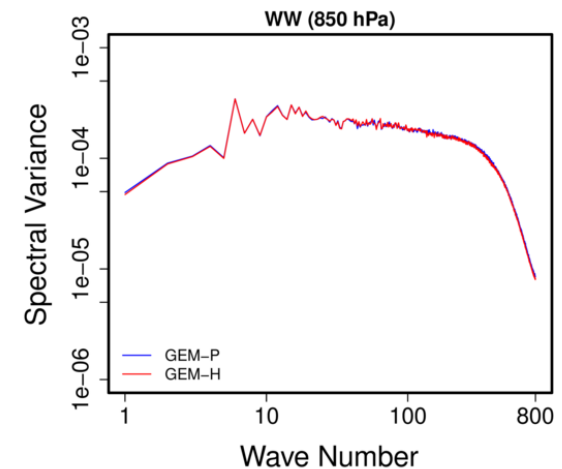
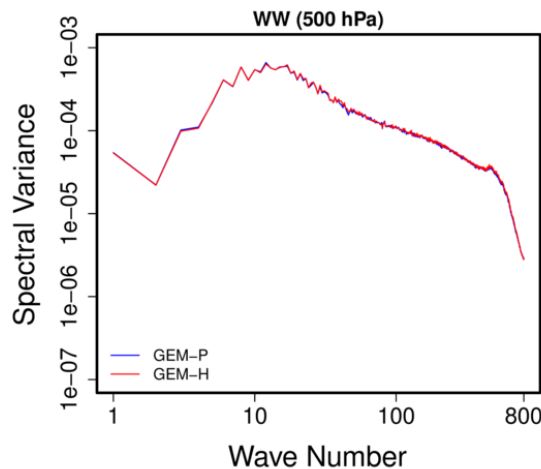
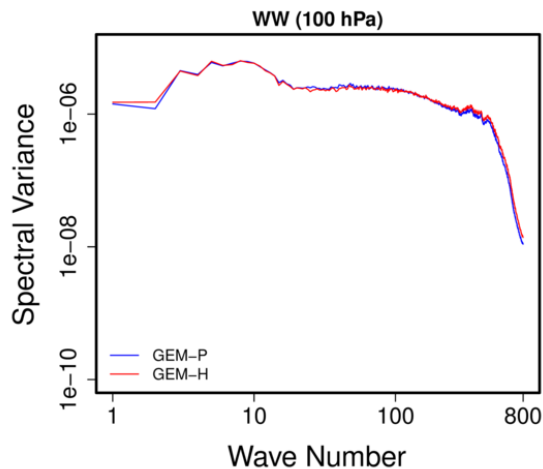
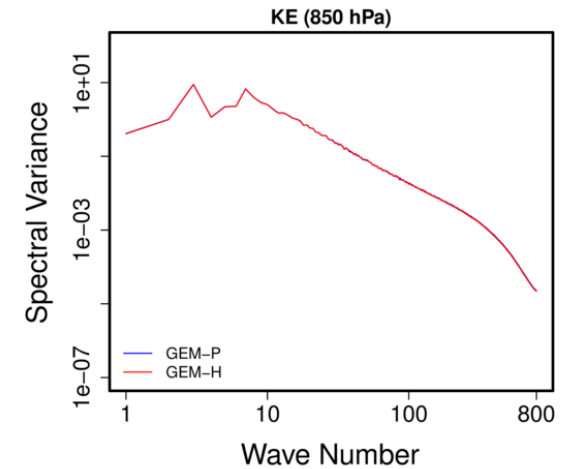
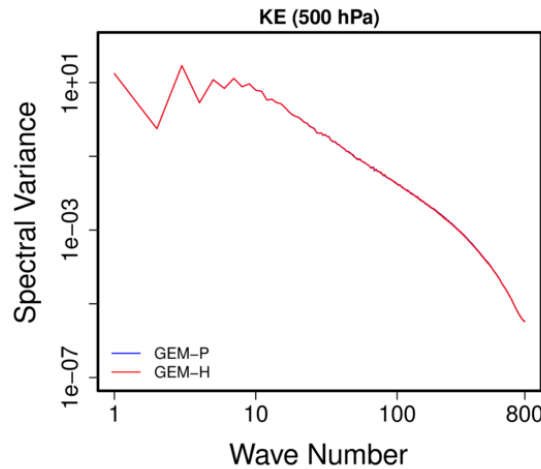
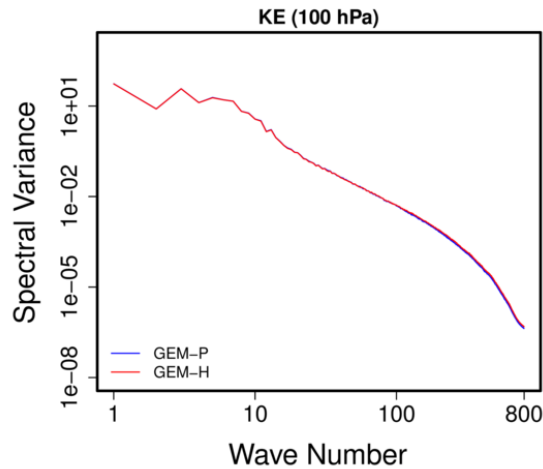


GZ: Geopotential height

TT: Temperature

Variance Spectra

GEM-P vs **GEM-H** (T+120 hr)

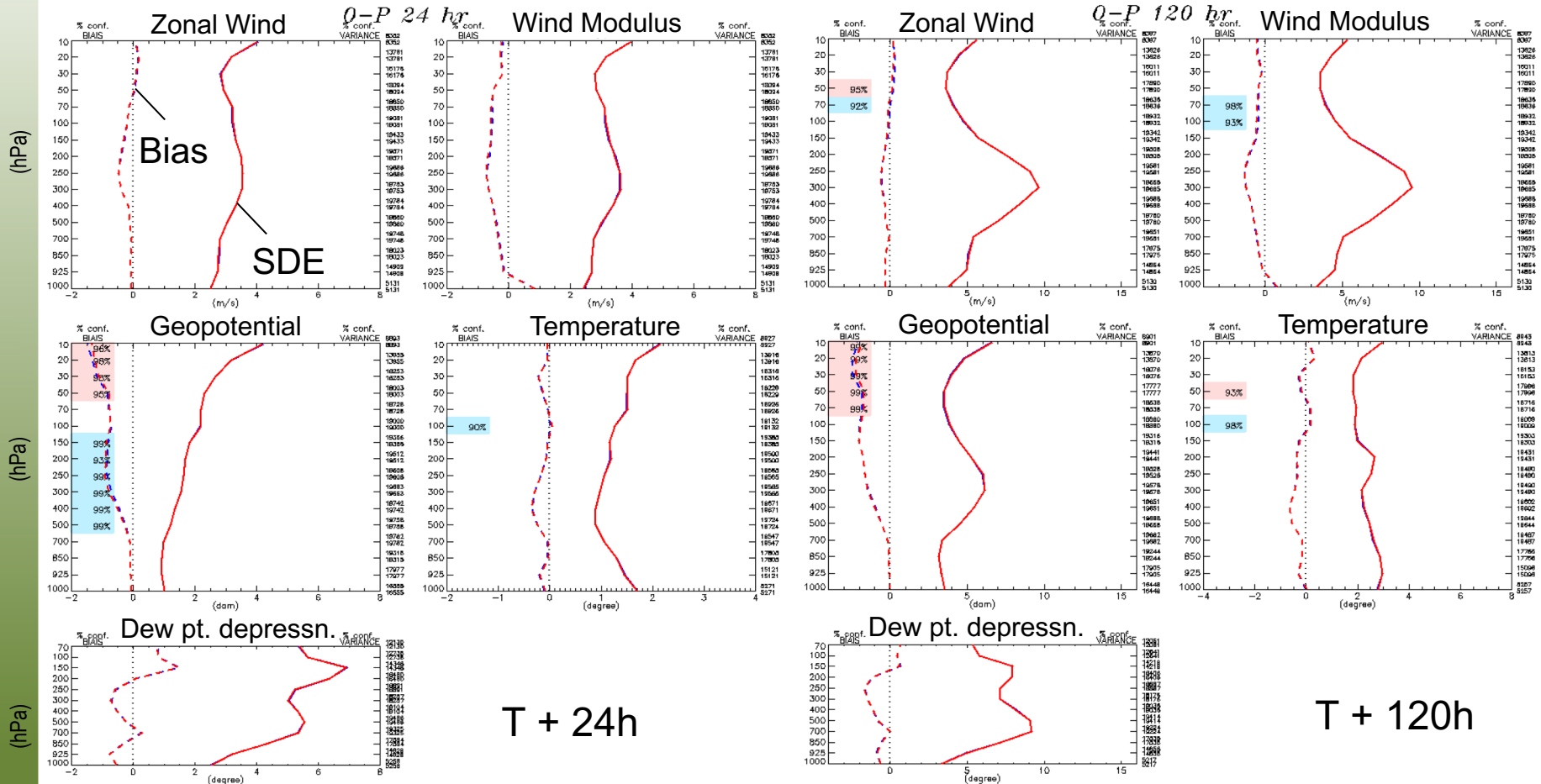


KE: Kinetic Energy

WW: Vertical Motion

Upper Air Scores

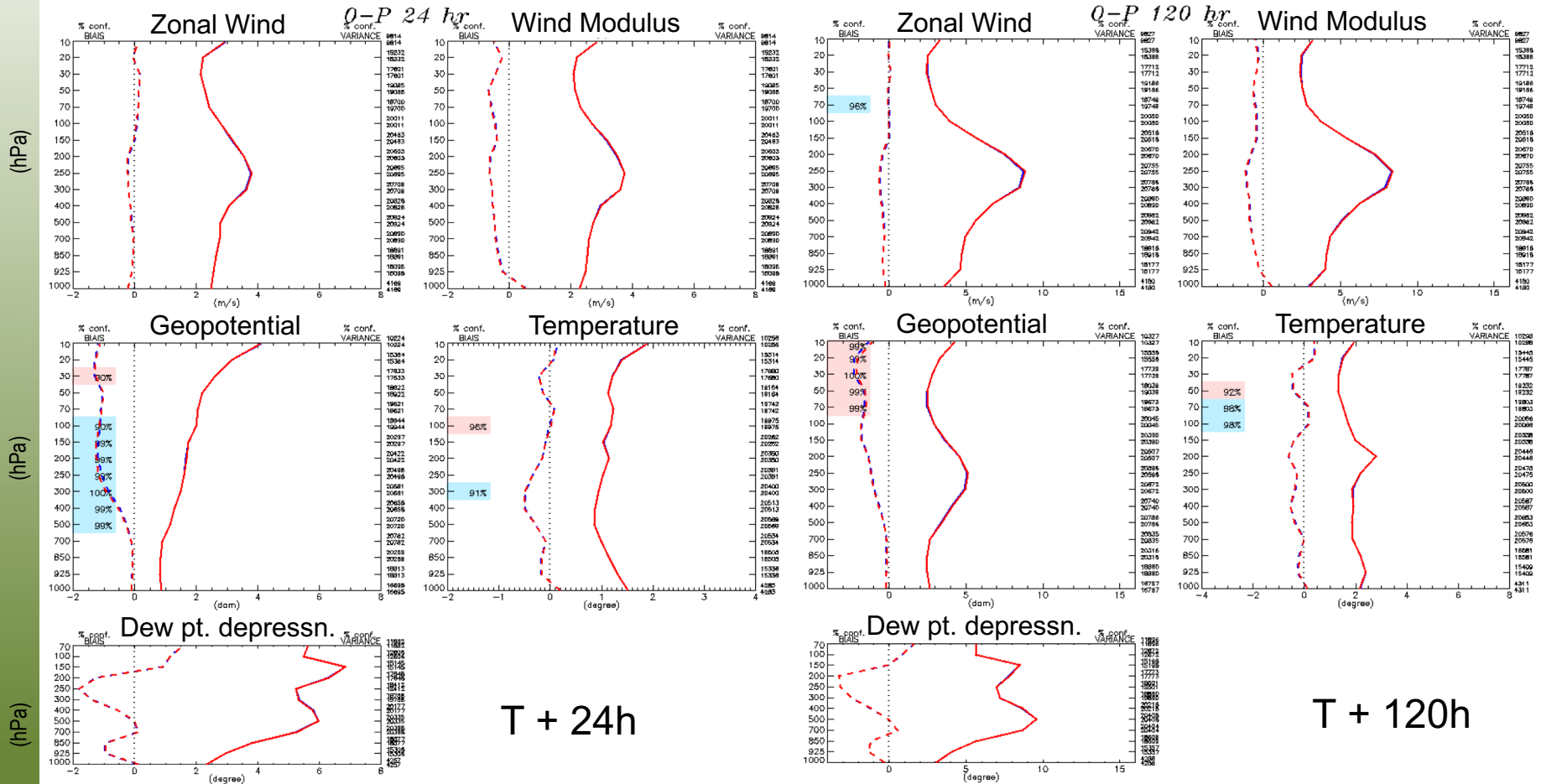
GEM-P vs GEM-H Winter 2015 (Global average of 44 cases)



*SDE: Standard Deviation of Error

Upper Air Scores

GEM-P vs GEM-H Summer 2014 (Global average of 44 cases)



T + 24h

T + 120h

Stability Comparison

GEM-P

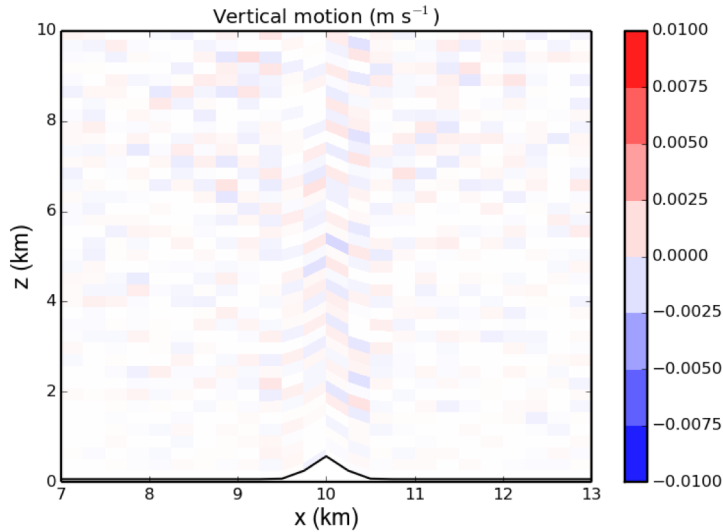
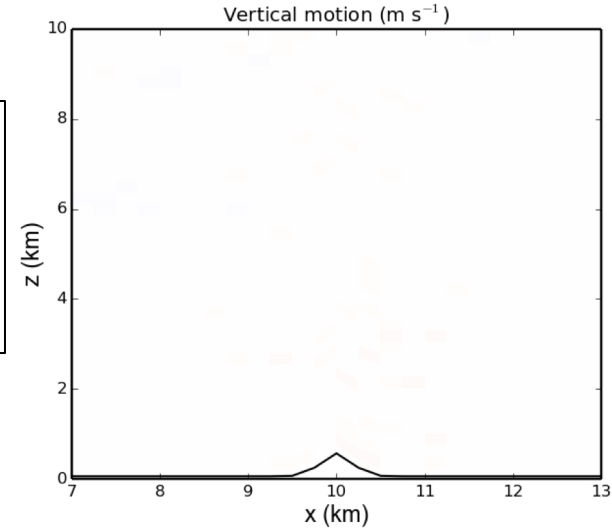


Fig. Vertical motion

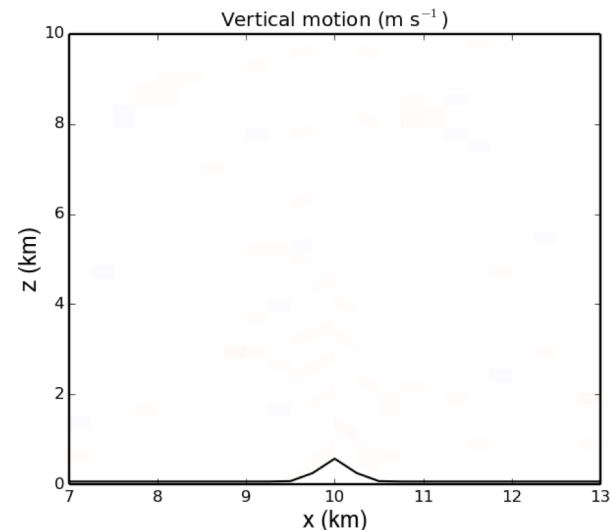
$H=500$ m
Max slope = 51.7°

$$b_m = b_h = b_{nh} = 0.6$$

GEM-H (direct)



GEM-H (iterative)



No flow case:

$\Delta x = \Delta z = 250$ m; $\Delta t = 10$ s

81 x 80 domain ($N_i \times N_k$)

Mountain height, H

$$z_s = H \exp[-\{(x-x_c)/a\}^2]$$

where $a = 1$ km

Stationary flow ($u=w=0$)

Initial temp. $T_0 = 260$ K

Ref. basic state temp. $T_* = 240$ K

Stability Comparison

GEM-P

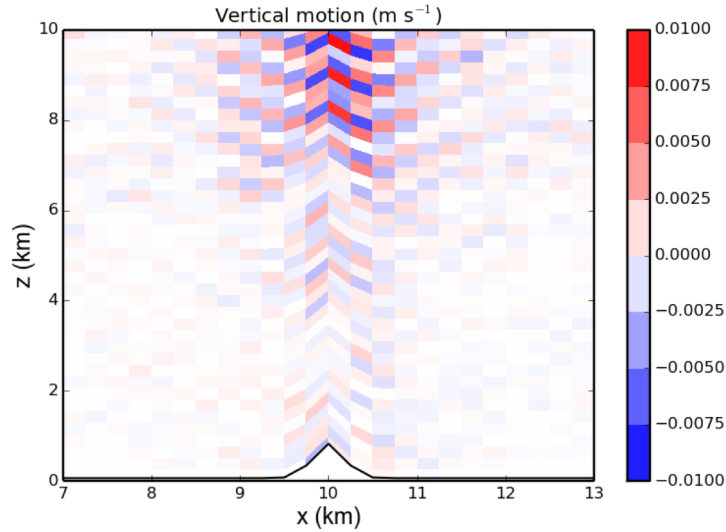
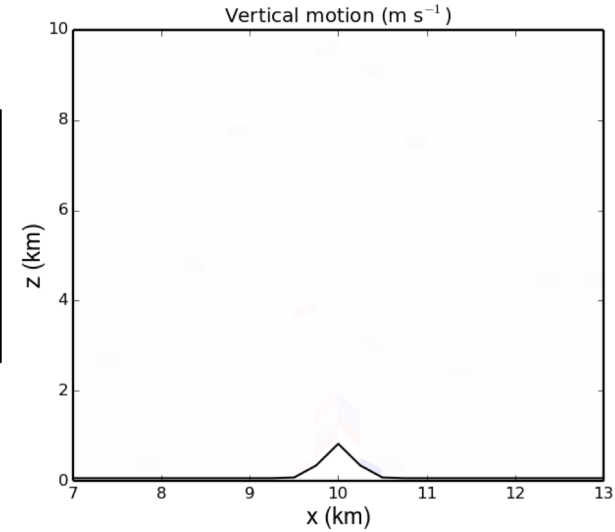


Fig. Vertical motion

H=750 m
Max slope = 62.2°

$$b_m = b_h = b_{nh} = 0.6$$

GEM-H (iterative)



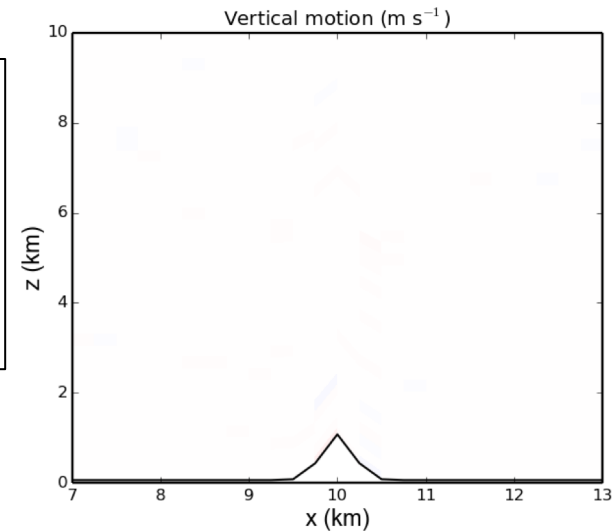
GEM-P



H=1000 m
Max slope = 68.4°

$$b_m = b_h = 0.6$$
$$b_{nh} = 0.75$$

GEM-H (iterative)



Summary

- The newly developed **GEM-H** dynamical core works for both global and limited-area prediction systems.
- Both direct and iterative solvers are functional for **GEM-H**.
- The RPN physics package has been coupled to the new dynamical core (without any additional calibration).
- For the theoretical cases as well as for 25-km global forecasts with **GEM-H** are found to be equivalent of **GEM-P**.
- Initial tests reveal the potential for **GEM-H** to improve stability over steep orography.
- The simplified approach for **GEM-H** that permits the use of the direct solver works as long as the slope is not too steep.



Environment and
Climate Change Canada

Environnement et
Changement climatique Canada

Canada 

Appendix



Environment and
Climate Change Canada

Environnement et
Changement climatique Canada

Canada 

Vertical Coordinates and Solvers: GEM-P vs GEM-H

General form of the EBV (for both **GEM-P** and **GEM-H**):

$$\nabla_H^2 P + M_{VH} P = R$$

where, the subscripts H and V indicate coefficients that vary in the horizontal and the vertical, and M_{VH} includes difference and mean operators in the horizontal and the vertical.

GEM-P

M_{VH} does not include horizontally variable coefficients. The EBV is vertically separable and solve using the fast **direct solver**.

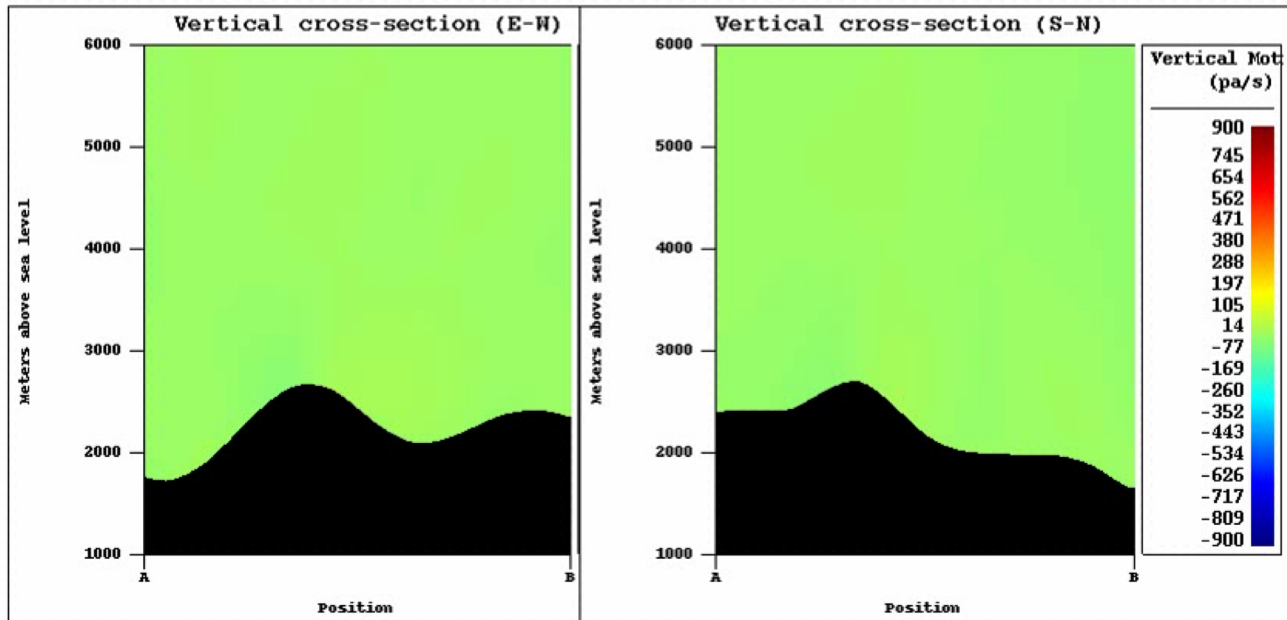
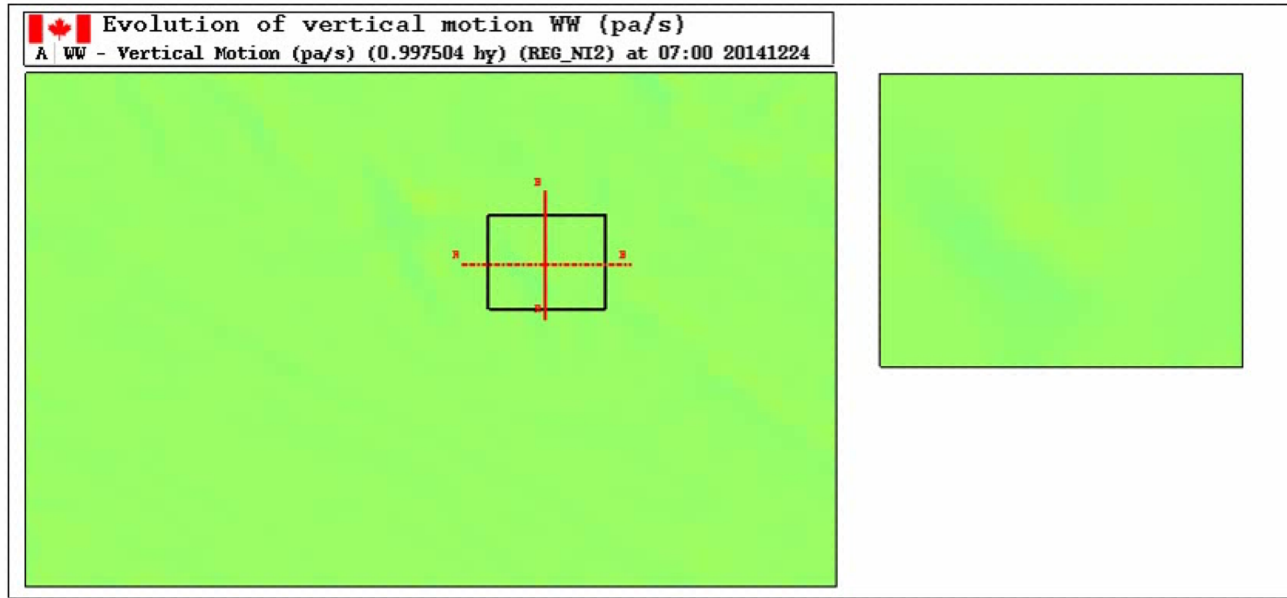
GEM-H

M_{VH} includes horizontally variable coefficients due to the metric terms (unless simplified). The EBV is not vertically separable and solve with an **iterative solver** (unless simplified).

The Solvers

- **Direct solver** is based on the generalized eigenvalue problem (Qaddouri and Lee, 2010).
 - The EBV problem is separated vertically in terms of the vertical eigenvalues of M_{VH} .
 - For N vertical levels, the resulting N number of vertically-decoupled 2D Helmholtz problems are solved using FFT to obtain the full 3D solution.
- **Iterative solver** is based on FGMRES (Qaddouri and Lee, 2010).
 - Solution vector minimizes the residual in a Krylov subspace.
 - Only needs to account for the action of the operator $(\nabla_H^2 + M_V)$ on the vector P (instead of generating the coefficient matrix).
 - Preconditioner is based on the block Jacobi solution of the elliptic problem in the absence of the metric terms.

Steep Orography-Induced Instability



Height-Based Vertical Coordinate

- The traditional definition of terrain-following height-based vertical coordinate ζ is given by

$$\zeta(z) = H \frac{z - z_S}{z_T - z_S}$$

where, z is the true height, the subscripts S and T denote surface and model top, respectively, and H is a normalizing constant.

- Assuming, $H = z_T = \zeta_T$, we get

$$z = A(\zeta) + B(\zeta)z_S$$

where, $A = \zeta$ and $B = \left(\frac{\zeta_T - \zeta}{\zeta_T}\right) = \lambda$.

- We have, $B = (\lambda)^r$, where $r = [r_{max} - (r_{max} - r_{min})\lambda]$.

Height-Based Vertical Coordinate

- This allows B to decrease more rapidly with height (if needed).
- **SLEVE**-like coordinate (Schär et al., 2002), defined as

$$z = \zeta + B_1 z_{sL} + B_2 (z_s - z_{sL})$$

is available, where z_{sL} stands for large-scale orography.

- **SLEVE** coordinate permits faster decrease of the effect of small-scale orography, i.e., $(z_s - z_{sL})$, on the model vertical coordinate with increasing height, and helps controlling computational noise in the upper troposphere and stratosphere.

Pressure-based Vertical Coordinate

- The current definition of vertical coordinate gives

$$\ln \pi = \zeta + Bs$$

where π is the hydrostatic pressure, ζ is the vertical coordinate, $s = \ln(\pi_s/p_{ref})$ with $p_{ref} = 10^5 \text{Pa}$ and B is a metric term to determine the flattening of the coordinate with height. Additionally,

$$B = \left(\frac{\zeta - \zeta_T}{\zeta_S - \zeta_T} \right)^r \text{ where } r = r_{max} - (r_{max} - r_{min})[(\zeta - \zeta_T)/\zeta_S - \zeta_T].$$

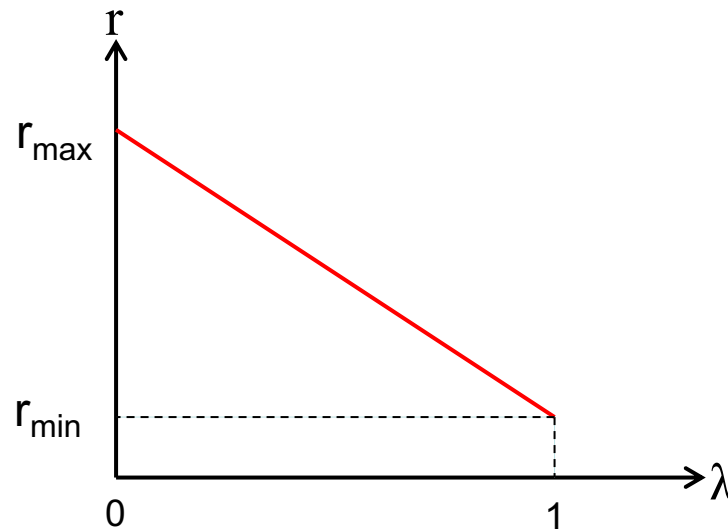
- Flattening is controlled by adjusting the values of r_{min} and r_{max} .



Height-Based Vertical Coordinate

- We have, $B = (\lambda)^r$, where $\lambda = \frac{\zeta_T - \zeta}{\zeta_T}$ and.
- This implies that at $\zeta = \zeta_S$, $\lambda = 1$ and at $\zeta = \zeta_T$, $\lambda = 0$.
- We want r to vary in such a way that when $\lambda = 1$, $r = r_{min}$ and $\lambda = 0$, $r = r_{max}$. This gives

$$r = [r_{max} - (r_{max} - r_{min})\lambda]$$



Final Dynamical System of Eqn.

Discretization in space leads to –

$$\frac{du}{dt} - \left(f + \frac{\tan\theta}{a} u \right) \bar{v}^{XY} + \frac{\bar{T}^{X\zeta}}{T_*} \left(\delta_X q - J_X \bar{J}_\zeta^{-1} \delta_\zeta q^{X\zeta} \right) = 0$$

$$\frac{dv}{dt} + \left(f + \frac{\tan\theta}{a} \bar{u}^{XY} \right) \bar{u}^{XY} + \frac{\bar{T}^{Y\zeta}}{T_*} \left(\delta_Y q - J_Y \bar{J}_\zeta^{-1} \delta_\zeta q^{Y\zeta} \right) = 0$$

$$\frac{dw}{dt} + \frac{T}{T_*} \left(J_\zeta^{-1} \delta_\zeta q - g \frac{T'}{T} \right) = 0$$

$$\frac{d}{dt} \left[\ln \left(\frac{T}{T_*} \right) - \frac{\bar{q}^\zeta}{c_p T_*} \right] + \mu w = 0$$

$$\frac{d}{dt} \left(\frac{q}{c_*^2} + \ln J_\zeta \right) + \delta_X u + \frac{1}{\cos\theta} \delta_Y (\cos\theta v) + \delta_\zeta \dot{\zeta} - \varepsilon \bar{w}^\zeta = 0$$

$$\frac{d}{dt} (z - \zeta) + \ddot{\zeta} - w = 0$$

where δ and $(\bar{\quad})$ denote difference and averaging operators.

Vertical Grid

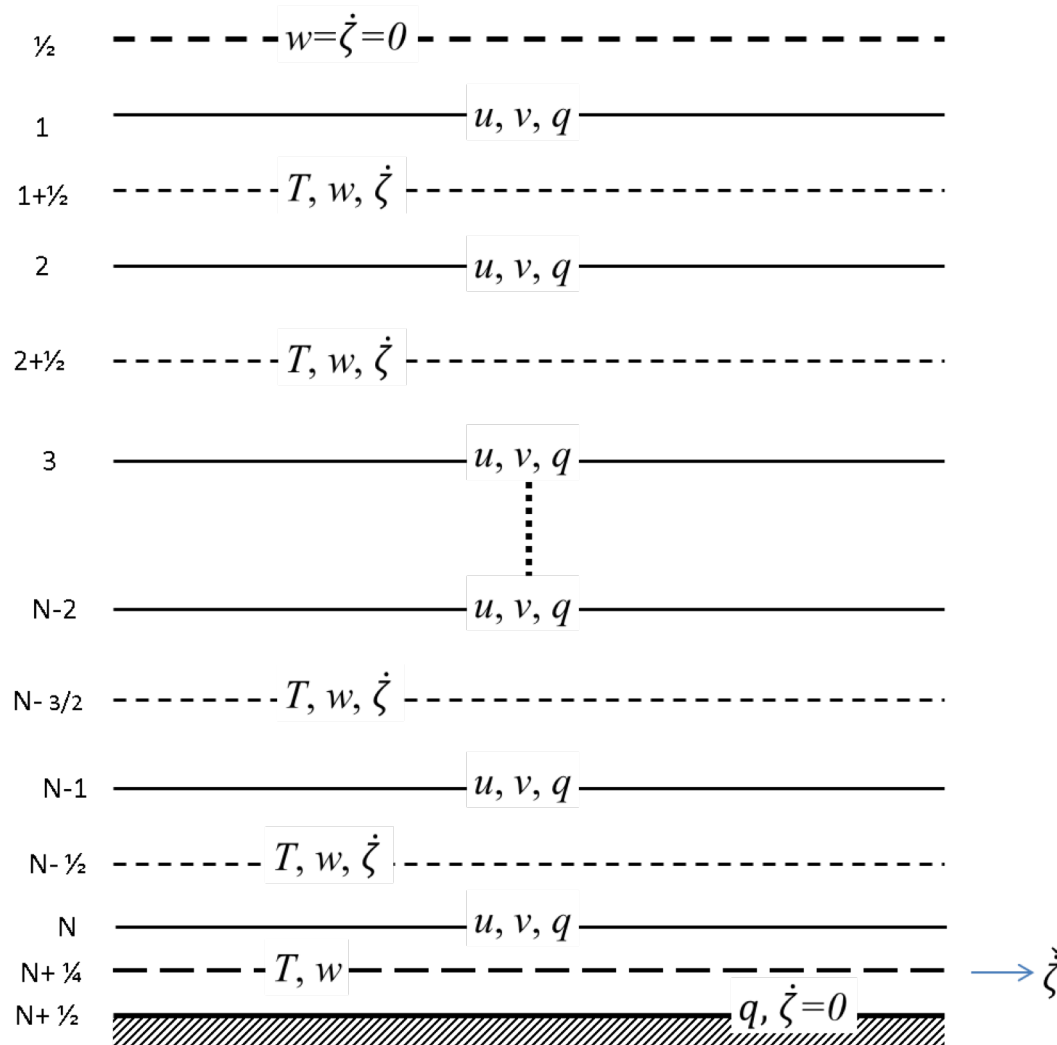


Fig. Vertical Charney-Phillips grid.

Horizontal Grid

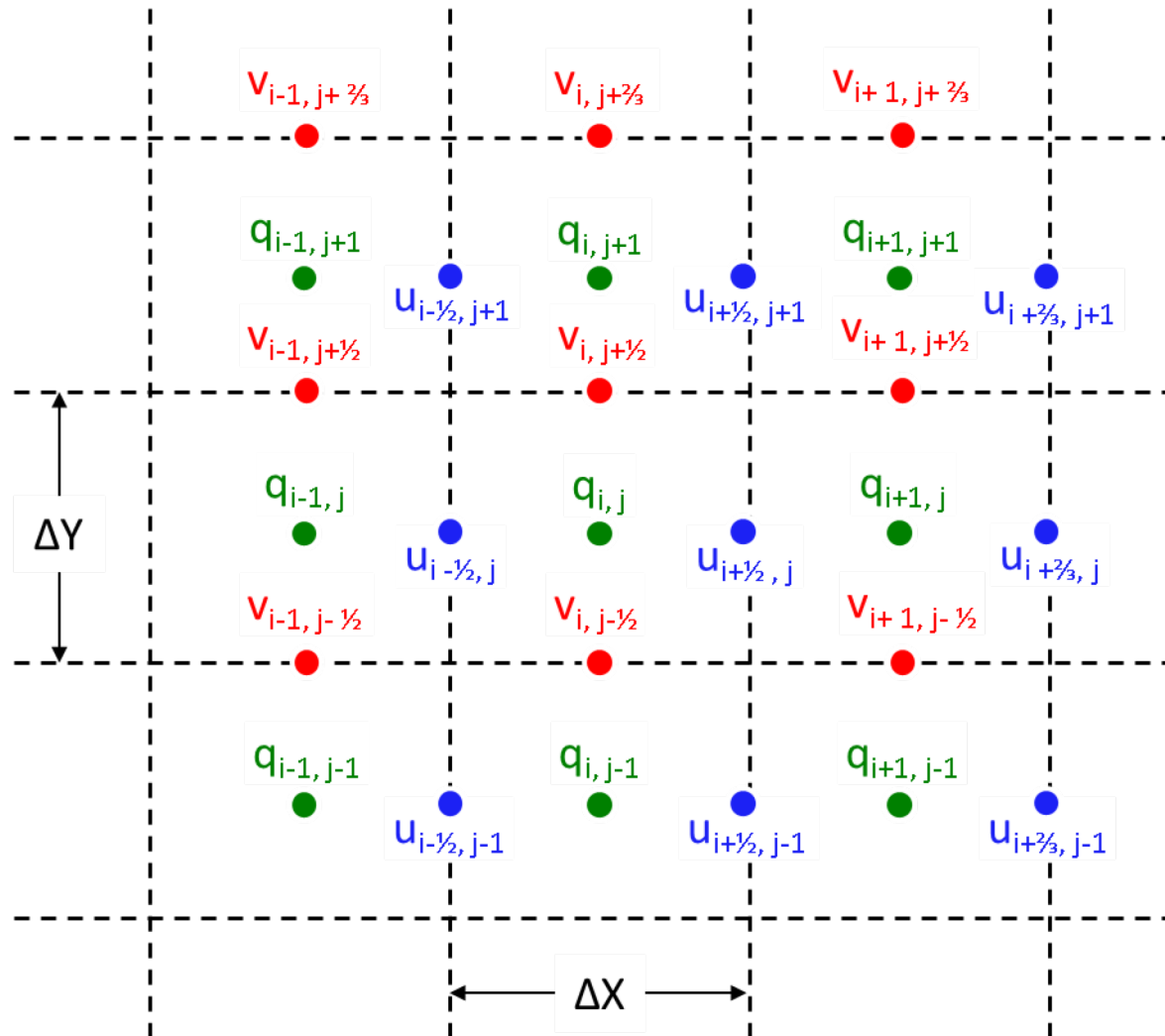


Fig. Horizontal Arakawa C grid.

Theoretical Test Cases

- At the early stage of development, the **GEM-H** dynamical core was tested against **GEM-P** for a number of theoretical cases to identify
 - possible issues around advection, and
 - its response to orography and nonhydrostatic scenario.
- Two of the theoretical cases were
 - Robert's bubble convection test (Robert, 1993) and
 - Schar's mountain wave case (Schär et al., 2002).

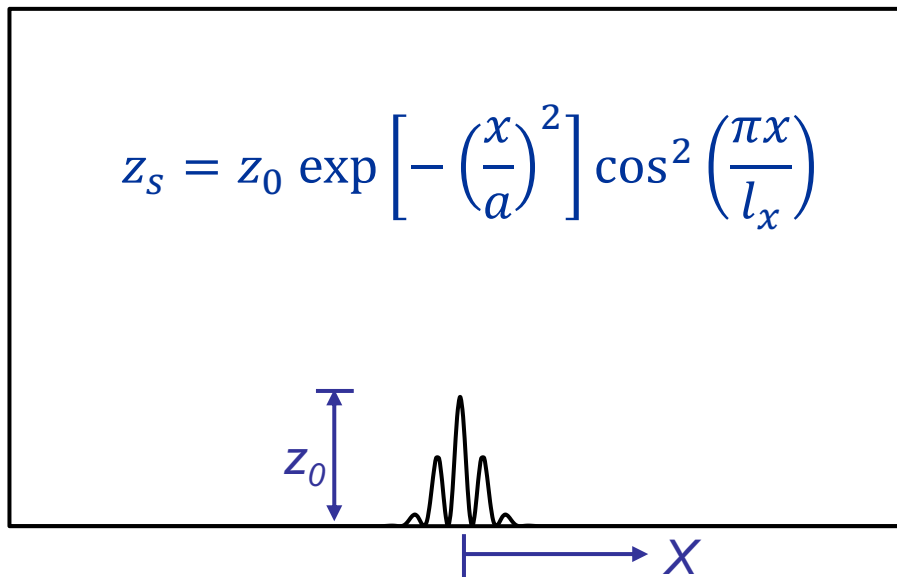
Robert, A. (1993): Bubble convection experiments with a semi-implicit formulation of the Euler equations. *J. of Atmos. Sciences*, 50: 1865-1873.

Schär, C., Leuenberger, D., Fuhrer, O., Lüthi, D., and Girard, C. (2002): A new terrain-following vertical coordinate formulation for atmospheric prediction models. *Mon. Wea. Rev.*, 130: 2459-2480.

The Schär Mountain Case

A Theoretical Non-Hydrostatic Case

Schär case: Dry flow past idealized topography



$$U = 10 \text{ ms}^{-1}$$
$$N = 0.01 \text{ s}^{-1}$$
$$T_\theta = 288 \text{ k}$$

$$L = 200 \text{ km} \quad H = 19.5 \text{ km}$$
$$N_f = 401 \quad N_k = 65$$
$$\Delta x = 500 \text{ m} \quad \Delta z = 300 \text{ m}$$
$$z_0 = 250 \text{ m} \quad a = 5 \text{ km}$$
$$l_x = 4 \text{ km} = 8 \Delta x$$

Schär, C., Leuenberger, D., Fuhrer, O., Lüthi, D., and Girard, C. (2002): A new terrain-following vertical coordinate formulation for atmospheric prediction models. *Mon. Wea. Rev.*, 130: 2459-2480.



2D Mountain Wave: Nonhydrostatic

- **Off-centering** leads to **perturbations** in both GEM-H and GEM-P.

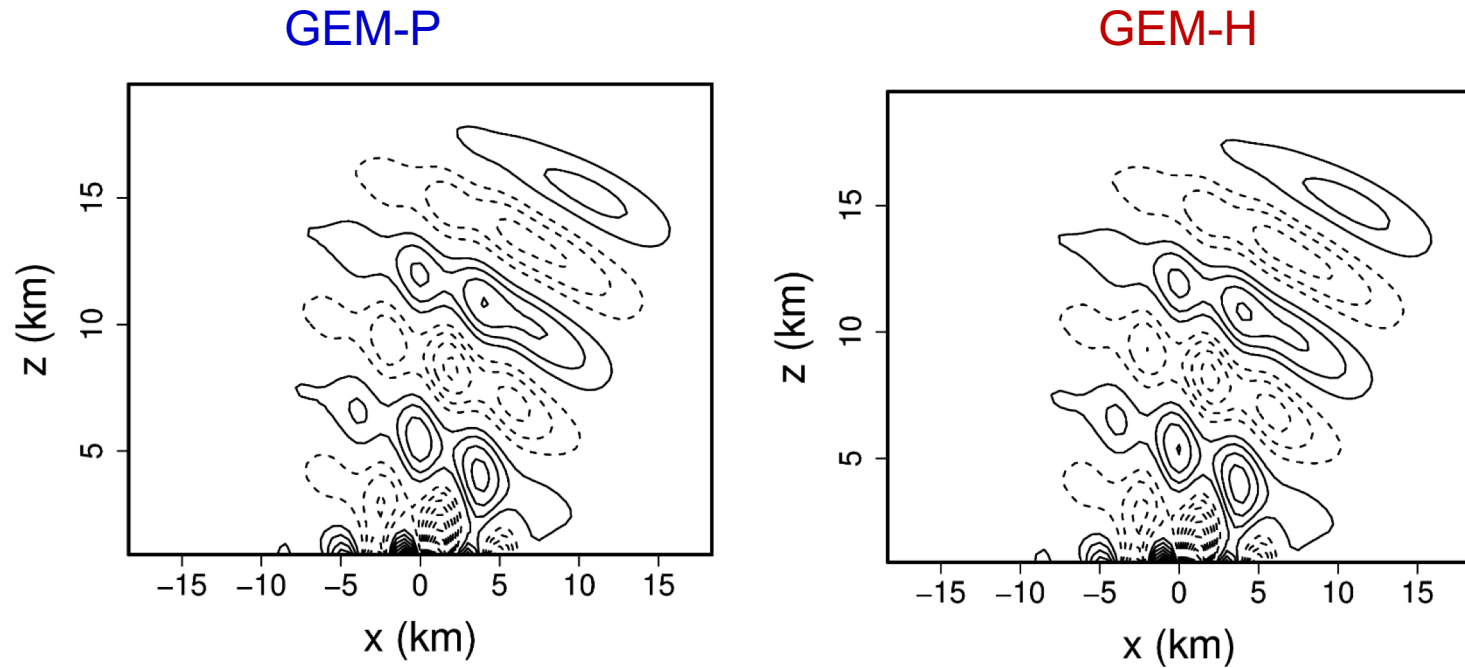


Fig: Vertical velocity contours with interval of 0.1 m s^{-1} ($b_A = 0.6$).

- Perturbations result from **inconsistent trajectory calculations** (Husain and Girard, 2017).

Husain, S.Z., and Girard, C. (2017): Impact of consistent semi-Lagrangian trajectory calculations on numerical weather prediction performance. *Mon. Wea. Rev.*, 145: 4127-4150.

2D Mountain Wave: Nonhydrostatic

- Problem is resolved with similar off-centering employed in the discretized trajectory equations.

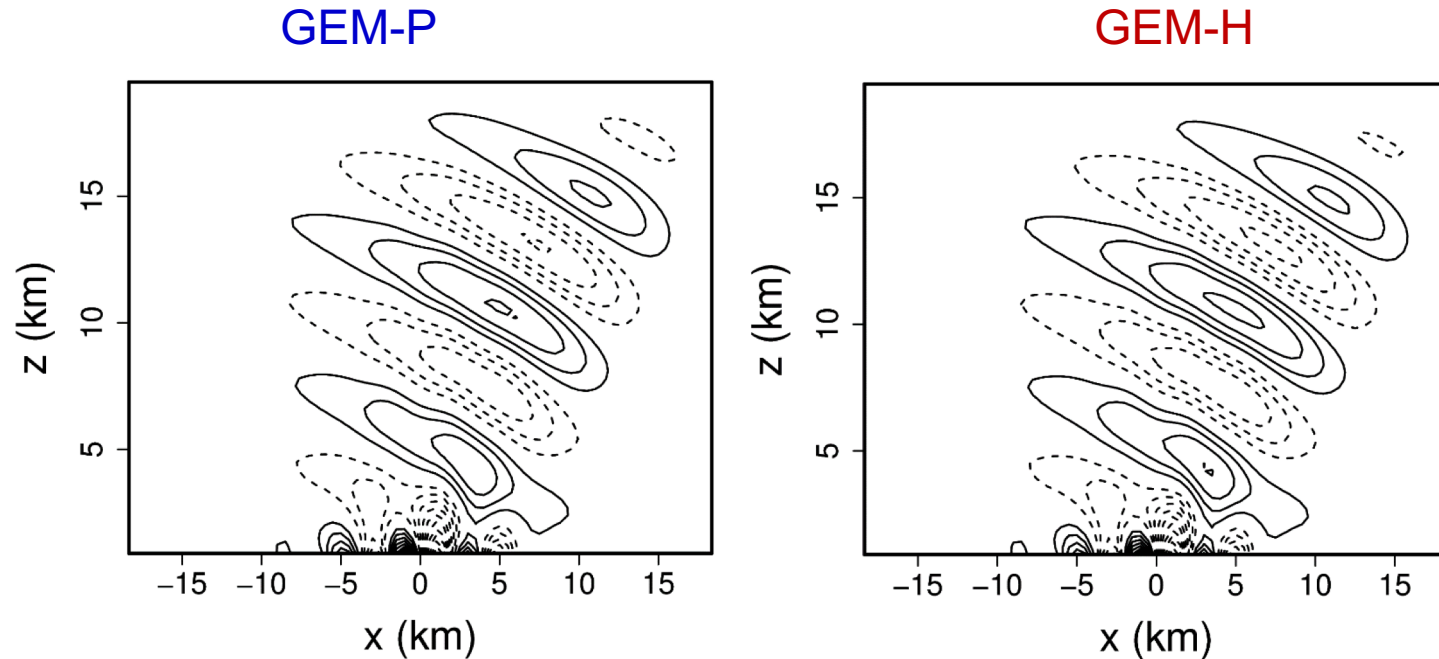
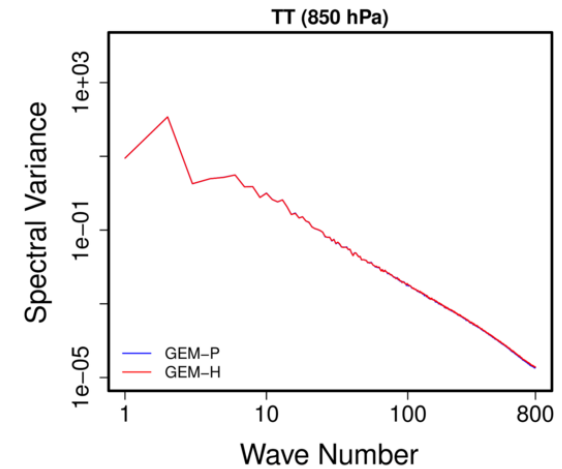
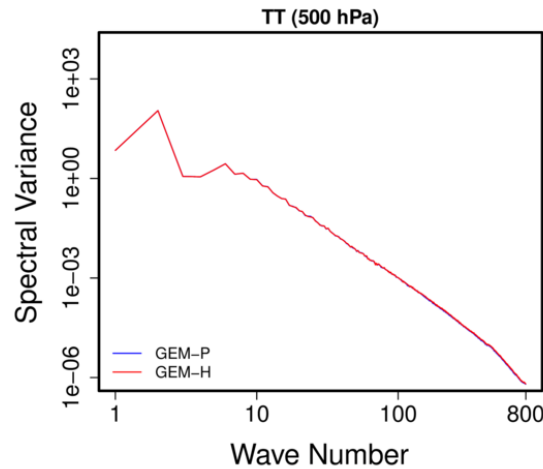
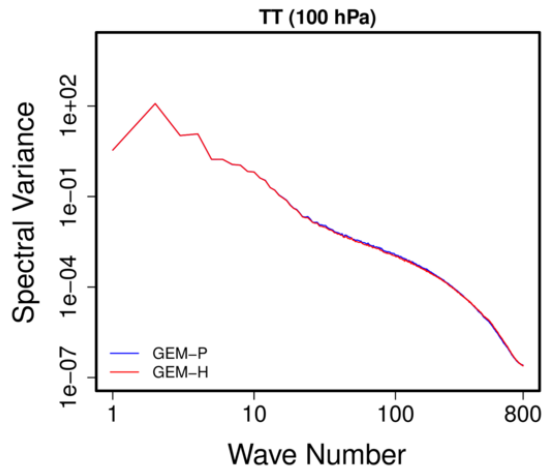
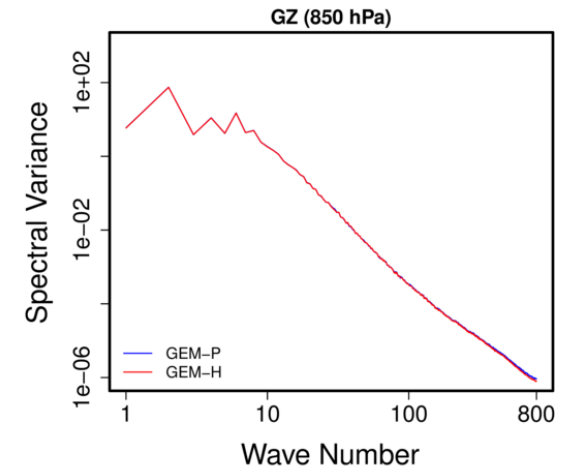
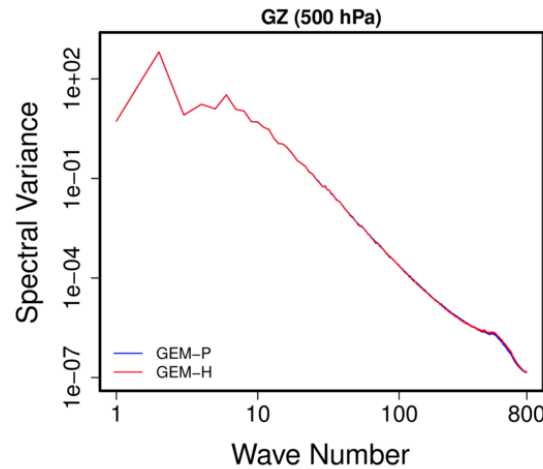
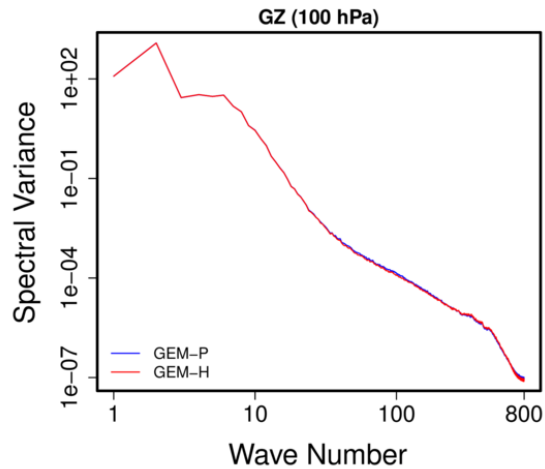


Fig: Vertical velocity contours with interval of 0.1 m s^{-1} ($b_A = 0.6$) with consistent trajectory calculations ($\text{Schm_advec} = 2$).

Variance Spectra

GEM-P vs **GEM-H** (T+120 hr)

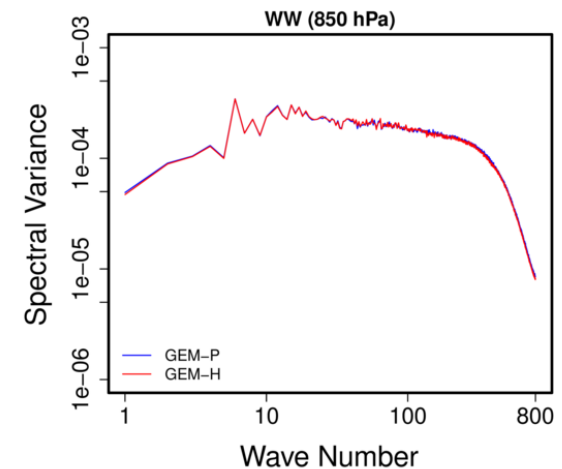
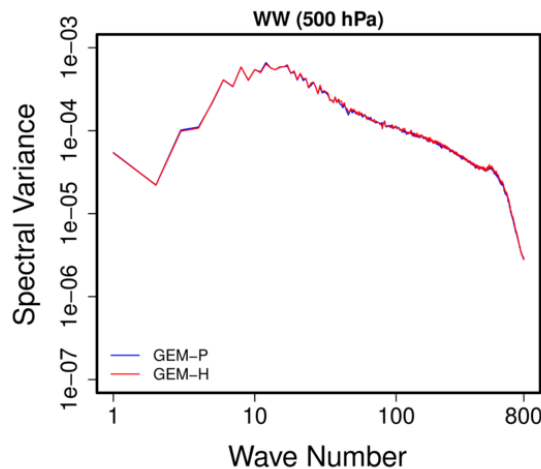
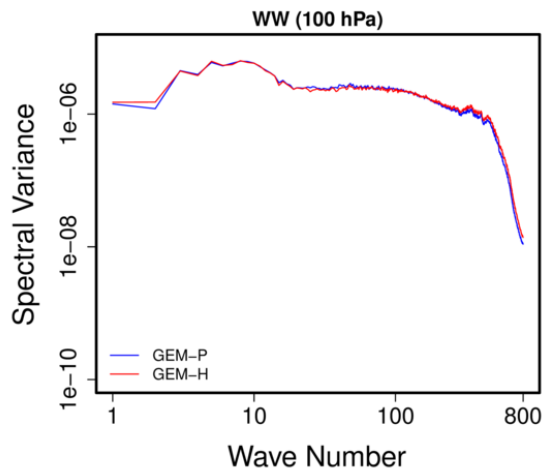
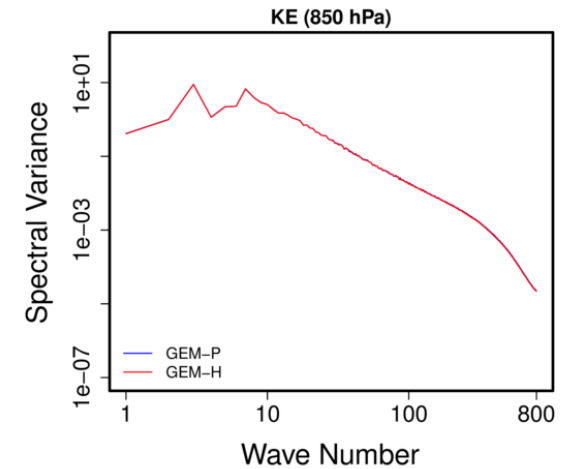
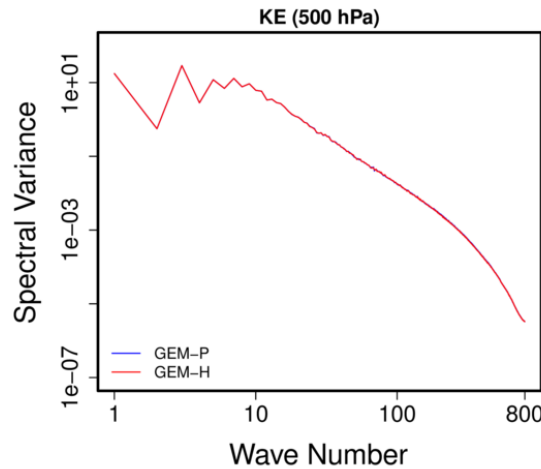
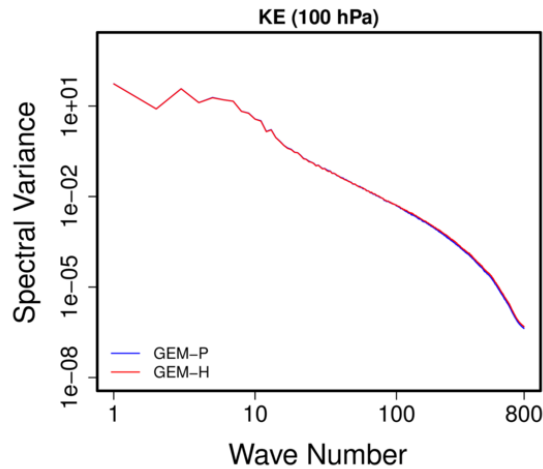


GZ: Geopotential height

TT: Temperature

Variance Spectra

GEM-P vs **GEM-H** (T+120 hr)



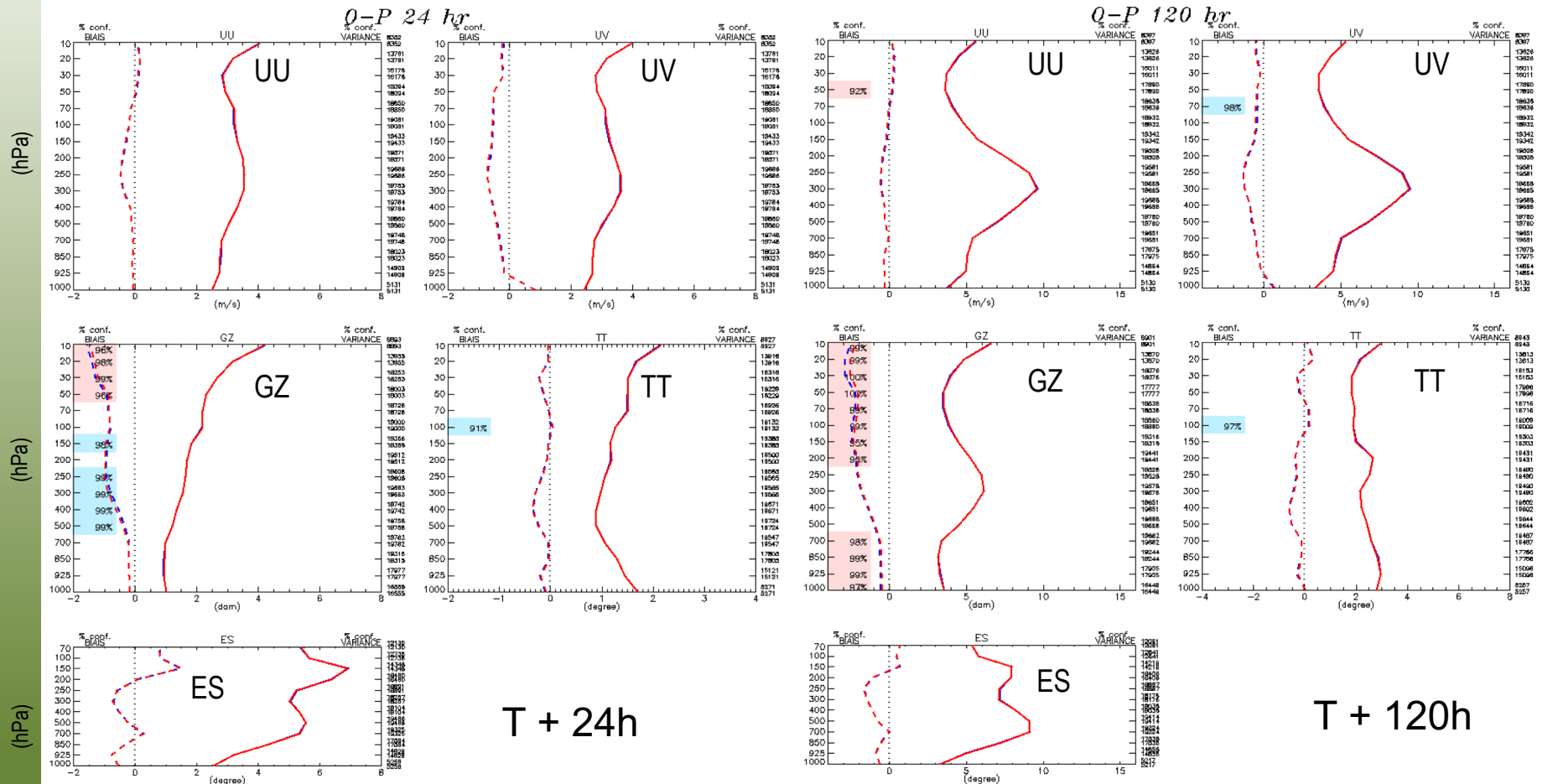
KE: Kinetic Energy

WW: Vertical Motion

Comparison Against Observations

GEM-P vs GEM-H

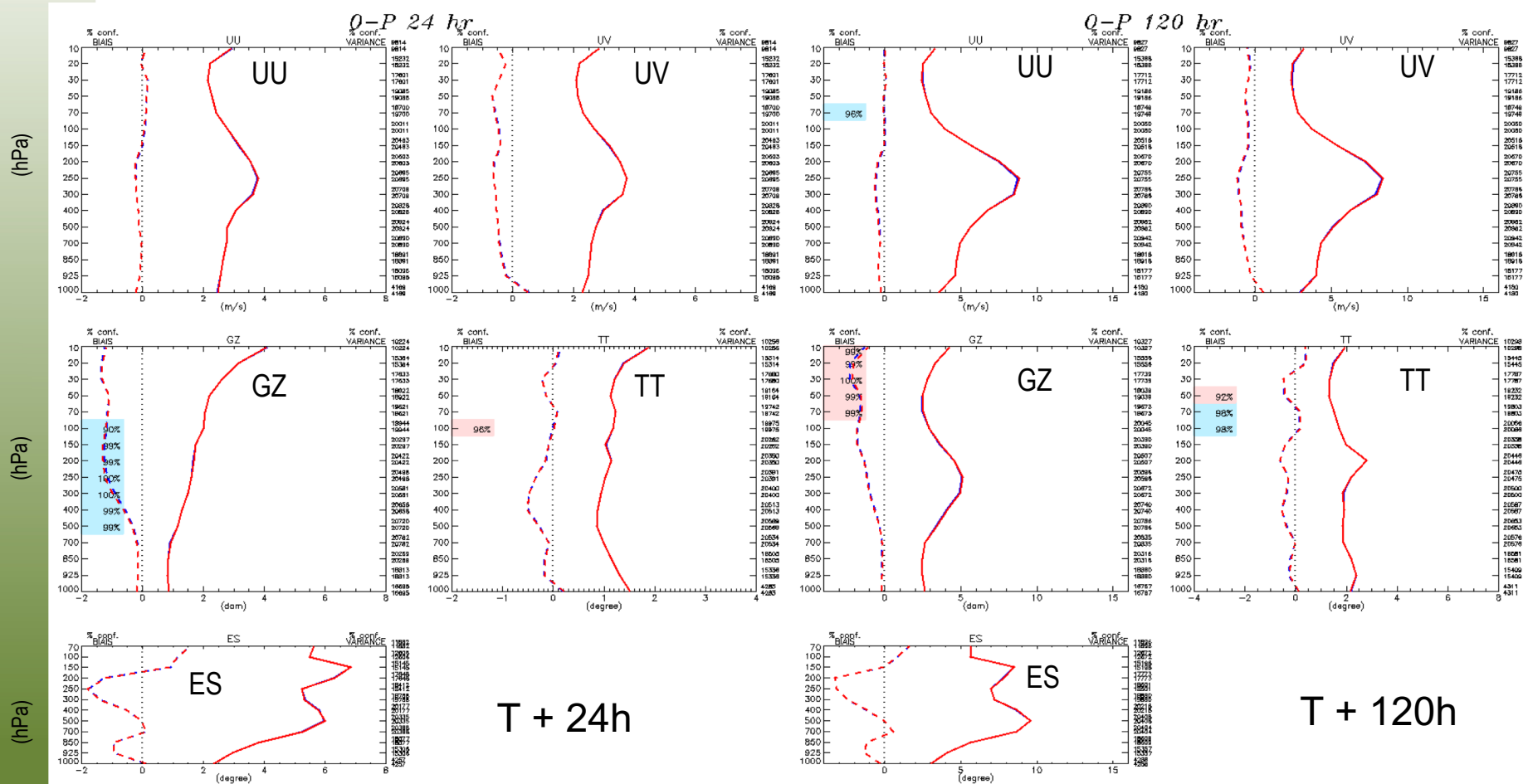
Winter 2015 (Global average of 44 cases)
Without mass fixer



UU: Zonal Wind, UV: Wind Speed, GZ: Geopotential Height, TT: Temperature, ES: Dew Point Depression

Comparison Against Observations

GEM-P vs GEM-H Summer 2014 (Global average of 44 cases) Without mass fixer



UU: Zonal Wind, UV: Wind Speed, GZ: Geopotential Height, TT: Temperature, ES: Dew Point Depression

Work in Progress

- **NWP:** Modifying and adapting the model code to permit **GEM-H** work with IAU, digital filter, etc.
- **Solver:** Developing highly optimized 3D iterative solvers for both **GEM-P** and **GEM-H**.
- **Stability:** Exploring strategies to improve stability of **GEM-H** over steep orography.
 - Initial tests revealed stability improvements with **GEM-H**.
 - Improved numerical approximation of horizontal gradients in the terrain-following coordinate (Zängl, 2012; Mahrer, 1984) may also be explored in **GEM-H**.

Zängl, G. (2012): Extending the numerical stability limit of terrain-following coordinate models over steep slopes. Mon. Wea. Rev., 140: 3722-3733.

Mahrer, Y. (1984): An improved numerical approximation of the horizontal gradients in a terrain-following coordinate system. Mon. Wea. Rev., 112: 918-922